Heterogeneous Tau-Tubulin Complexes Accelerate Microtubule Polymerization

Xiao-Han Li[1] and Elizabeth Rhoades[2,*]

[1]Department of Chemistry, Yale University, New Haven, Connecticut and [2]Department of Chemistry, University of Pennsylvania, Philadelphia, Pennsylvania

ABSTRACT   Tau is an intrinsically disordered protein with a central role in the pathology of a number of neurodegenerative diseases. Tau normally functions to stabilize neuronal microtubules, although the mechanism underlying this function is not well understood. Of note is that the interaction between tau and soluble tubulin, which has implications both in understanding tau function as well as its role in disease, is underexplored. Here we investigate the relationship between heterogeneity in tau-tubulin complexes and tau function. Specifically, we created a series of truncated and scrambled tau constructs and characterized the size and heterogeneity of the tau-tubulin complexes formed under nonpolymerizing conditions. Function of the constructs was verified by tubulin polymerization assays. We find that, surprisingly, the pseudo-repeat region of tau, which flanks the core microtubule-binding domain of tau, contributes largely to the formation of large, heterogeneous tau tubulin complexes; additional independent tubulin binding sites exist in repeats two and three of the microtubule binding domain. Of particular interest is that we find positive correlation between the size and heterogeneity of the complexes and rate of tau-promoted microtubule polymerization. We propose that tau-tubulin can be described as a "fuzzy" complex, and our results demonstrate the importance of heterogeneous complex formation in tau function. This work provides fundamental insights into the functional mechanism of tau, and more broadly underscores the relevance of heterogeneous and dynamic complexes in the functions of intrinsically disordered proteins.

INTRODUCTION

Tau is a microtubule-associated protein (MAP) that has a central role in the pathology of a group of neurodegenerative disorders including Alzheimer's disease and traumatic brain injury, collectively known as tauopathies (1,2). The major functions of tau are to stabilize microtubules and promote their assembly (3,4). Both gain-of-toxicity and loss-of-normal-function are thought to contribute to the development of tauopathies (5).

Tau is an intrinsically disordered protein in that it lacks stable secondary structure and tertiary interactions. Tau consists of three major regions: 1) the highly disordered N-terminal domain that projects away from microtubule surface and has been proposed to play a role in spacing of microtubules (6); 2) the proline-rich region that enhances microtubule binding (7–9); and 3) the microtubule binding region (MTBR) that directly mediates the interaction with microtubules (10). The MTBR consists of either three (3R) or four (4R) imperfect repeats—R1, R2, R3, and R4—linked by three inter-repeat (IR) sequences, $IR_{1/2}$, $IR_{2/3}$, and $IR_{3/4}$;

3R tau isoforms lack $IR_{1/2}$-R2 (Fig. 1 A). Previous studies suggest each repeat region binds weakly to the microtubule lattice whereas sequences flanking the MTBR form a jaw-domain to enhance microtubule binding (9–11). It has also been proposed that the inter-repeats/repeats bind independently but unevenly to microtubules, with R1–R2 and R1–R3 accounting for most of the interaction energy for 4R and 3R isoforms of tau, respectively (12,13).

Although extensive biochemical and biophysical investigations have made significant contributions to understanding tau's interactions with microtubules, much less attention has been given to soluble tubulin as a functional binding partner for tau. Recent work from our lab demonstrated that tau binds with comparable—or greater—affinity to soluble tubulin than stabilized microtubules (14), emphasizing the potential importance of this interaction in tau function. We also found that tau can bind to multiple tubulin dimers, even under conditions where tubulin polymerization is inhibited, and that it mediates both lateral and longitudinal interactions between tubulin dimers (15). This is consistent with other reports of tau cross-linking dimers longitudinally (16,17). Moreover, we have suggested that there may be a hierarchy among the repeat regions for binding to tubulin, with R3 dominating the interaction (14,15). However, the
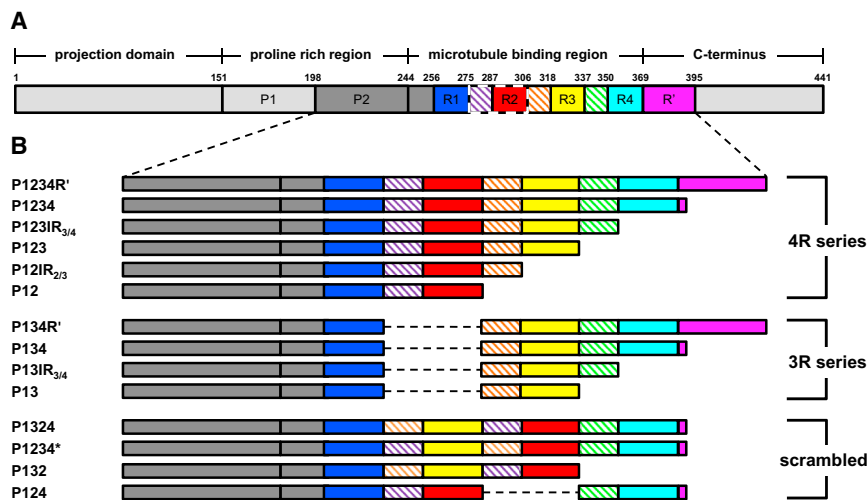
A

B

FIGURE 1 Schematics of tau constructs. (*A*) Given here is the longest isoform of human tau. The regions of interest are color-coded: P2, dark gray; R1, blue; $IR_{1/2}$, purple; R2, red; $IR_{2/3}$, orange; R3, yellow; $IR_{3/4}$, green; R4, cyan; and R′, magenta. The inter-repeats are indicated by hatch marks. $IR_{1/2}$–R2, highlighted by dashed lines, is alternatively spliced to generate 3R/4R tau. The numbers on top of the schematic indicate residues delineating both major domains and subdomains of interest to this study. (*B*) Given here are the constructs used in this work. The color-code for each construct matches that in (*A*). Gray dashed lines indicate deletion of specific subdomains.

molecular details and functional consequences of our model require further exploration.

Here, we investigate the contributions of the individual inter-repeats/repeats and the pseudo-repeat region (R′: Fig. 1) of tau to binding to soluble tubulin. We created 14 tau constructs based on truncation and scrambling of the repeat and inter-repeat regions within both 3R and 4R tau (Fig. 1). Fluorescence correlation spectroscopy (FCS) was used to assess the size of tau-tubulin complexes, revealing heterogeneity in these complexes, with increasing heterogeneity corresponding to an increase in the number of binding repeats. Moreover, we discovered a strong correlation between the complex stoichiometry and the ability of tau to promote microtubule assembly. We propose that tau-tubulin forms a "fuzzy complex" and our results highlight the importance of this binding heterogeneity in tau function.

MATERIALS AND METHODS

Purification and labeling of tau constructs

Tau was purified via an N-terminal His-tag as described in Elbaum-Garfinkle et al. (14). The His-tag was subsequently removed by TEV protease and the protein further purified by size exclusion chromatography. For fluorescent labeling with Alexa 488 maleimide, a cysteine was introduced at the N-terminus of each tau construct. See Supporting Material for details.

Tubulin purification

Tubulin was purified from fresh bovine brains as described in Li et al. (15) and Castoldi and Popov (18). See Supporting Material for details.

FCS

FCS measurements were performed on a lab-built instrument utilizing an IX-71 microscope (Olympus, Melville, NY) (15). All measurements were performed in phosphate buffer (20 mM potassium phosphate, 20 mM KCl, 1 mM $MgCl_2$, 0.5 mM EGTA, pH 7.4) at 20°C. Unless noted, tau-

tubulin complex measurements contained 20 nM tau and 20 μM tubulin to ensure saturation of binding.

Microtubule polymerization

Microtubule polymerization was monitored via light scattering at 350 nm as described in Elbaum-Garfinkle et al. (14). Polymerization assays were carried out at 37°C in BRB80 buffer (80 mM PIPES, pH 6.8, 1 mM $MgCl_2$, 1 mM EGTA) with 1 mM DTT freshly added. See Supporting Material for details.

Sequence analysis

Sequences for R1, R2, R3, R4, and R′ were analyzed by the webserver CIDER (19) to extract charge profile information. See Supporting Material for details.

RESULTS

Tau-tubulin complexes are heterogeneous

FCS measurements were carried out under nonpolymerizing conditions using fluorescently labeled tau in the presence of an excess of tubulin. For P1234R′-tubulin, repeated autocorrelation curves of the same sample are heterogeneous (Fig. S1). This is in contrast to FCS measurements of P1234R′ in the absence of tubulin, where the autocorrelation curves of repeated measurements are superimposable (Fig. S1). To analyze the heterogeneity, we fit individual curves and plotted the distribution of diffusion times. This distribution was fit with a Gaussian function and the width of the distribution was used to quantify the heterogeneity of the complexes (see Supporting Material for details of this analysis). The median diffusion time for P1234R′-tubulin, 0.87 ms, is significantly higher than tau or tubulin alone (Fig. 2; Table 1; Table S1), consistent with our previous results (15). Interestingly, the tau-tubulin complexes exhibited a very wide distribution of diffusion times with a peak width of 0.33 ms, indicating that tau-tubulin
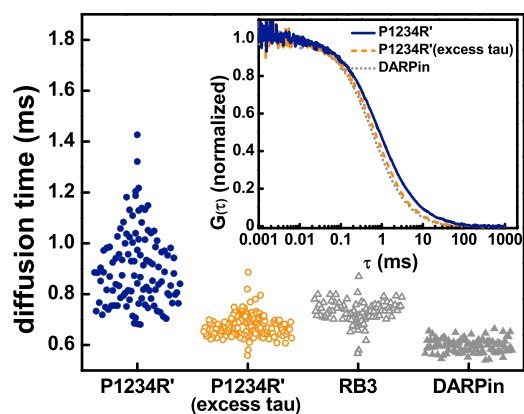
FIGURE 2 Heterogeneity of tau-tubulin complexes. Shown here is the distribution of the diffusion times derived from fits of individual autocorrelation curves. (*Inset*) Given here are normalized average autocorrelation curves of P1234R′-tubulin with excess tubulin or excess tau and DARPin-tubulin. To see this figure in color, go online.

complexes are heterogeneously sized and thus have variable tau-tubulin stoichiometry. Although these complexes are large, there is no evidence of polymerization (Fig. S2). Moreover, the autocorrelation curves from a FCS measurement of a 20 μM sample of tubulin in the absence of tau do not show evidence of such heterogeneity, indicating that it is specific to tau-tubulin (Fig. S3).

The engineered proteins DARPin (20) and RB3 (21–23) bind to tubulin with 1:1 and 1:2 (construct:tubulin dimer) stoichiometries. As such, their measurement by FCS allowed for the establishment of diffusion times of these well-defined complexes for comparison with tau-tubulin. The median diffusion times were 0.60 and 0.73 ms, respec-

tively, for DARPin-tubulin and RB3-tubulin. Moreover, both DARPin-tubulin and RB3-tubulin have narrow distributions of diffusion times with peak widths of 0.07 and 0.08 ms, respectively (Fig. 2; Table 1). The observation is consistent with homogeneous protein complexes with well-defined stoichiometry and is in stark contrast to our observation for tau-tubulin. Through comparison of distribution of diffusion times of P1234R′-tubulin with these two controls, it is apparent that under conditions of excess tubulin, P1234R′ binds to multiple tubulins and with variable stoichiometry.

To determine the impact of tubulin concentration on the size of tau-tubulin complexes, measurements were made with labeled tubulin (20 nM) and unlabeled tau (20 μM) (see Supporting Material for details). The median diffusion time of the complex under these conditions is 0.67 ms with a peak width of 0.09 ms (Fig. 2; Table 1). The diffusion time is slightly longer than that of DARPin-tubulin, as is expected, given that P1234R′ is larger than DARPin (201 residues as compared to 169 residues). Moreover, whereas DARPin is globular and compact, P1234R′ is mostly disordered when bound and, as a consequence, more extended (15,24) (Fig. S4; Table S1). These measurements are all consistent with a 1:1 tau-tubulin complex when tau is in great excess of tubulin. The 1:1 complexes formed when tubulin is the limiting binding partner provide a direct contrast to the larger, heterogeneous complexes measured when tubulin is in excess. These measurements also suggest that changes in accessible concentrations of either tau or tubulin could regulate the nature of the complexes formed in the cellular context as well.

TABLE 1 FCS and Polymerization Parameters for Tau Constructs

Construct		Length	Diffusion Time (ms)		Polymerization ($\pm$ SD)	
			Median	Peak Width	$t_{1/2}$ (s)	k_{obs} ($\times 10^{-2}$ s^{-1})
4R	P1234R	201	0.87	0.33	32 $\pm$ 2	3.1 $\pm$ 0.2
			0.67 (excess tau)	0.09		
	P1234	179	0.75	0.15	64 $\pm$ 12	1.6 $\pm$ 0.3
	P123IR$_{3/4}$	156	0.67	0.12	111 $\pm$ 14	0.9 $\pm$ 0.1
	P123	143	0.69	0.12	91 $\pm$ 9	1.1 $\pm$ 0.1
	P12IR$_{2/3}$	124	0.63	0.10	444 $\pm$ 43	0.22 $\pm$ 0.02
	P12	112	0.60	0.07	852 $\pm$ 86	0.12 $\pm$ 0.01
			0.61 (excess tau)	0.08		
3R	P134R′	170	0.79	0.23	50 $\pm$ 7	2.0 $\pm$ 0.3
	P134	148	0.65	0.08	321 $\pm$ 17	0.32 $\pm$ 0.02
	P13IR$_{3/4}$	125	0.66	0.09	765 $\pm$ 104	0.13 $\pm$ 0.02
	P13	112	0.60	0.09	350 $\pm$ 44	0.29 $\pm$ 0.04
			0.60 (excess tau)	0.07		
Scrambled	P1324	179	0.74	0.15	50 $\pm$ 6	2.0 $\pm$ 0.2
	P1234*	179	0.76	0.12		
	P132	143	0.72	0.15	—	—
	P124	148	0.65	0.09	—	—
Controls	DARPin	169	0.60	0.07		
	RB3	147	0.73	0.08		
	tubulin	—	0.52	0.08		
			0.54 (+20 μM tubulin)	0.08		

R′ enhances heterogeneity of tau-tubulin complexes

To assess how individual subdomains in the MTBR contribute to tubulin binding, P1234R′ was stepwise truncated from R′ to the reported microtubule binding core, P12 (Fig. 1) (13). FCS measurements were made in the presence of excess tubulin. With removal of R′, both the distribution median and the width decreased to 0.75 and 0.15 ms, respectively, from 0.87 to 0.33 ms (Fig. 3; Table 1). The striking downshift of both median diffusion time and width of the distribution suggests that R′ binds to tubulin and increases the stoichiometry of the tau-tubulin complex. The stepwise removal of R4, IR$_{3/4}$, and R3 further decreases the median diffusion times with negligible changes in the peak widths (Fig. 3; Table 1). Finally, removal of IR$_{2/3}$, to generate P12, results in another decrease in median diffusion time to 0.60 ms (Fig. 3; Table 1).

To put the extent of heterogeneity in the tau-tubulin complexes in context, they are considered in comparison to 1:1 tau-tubulin complexes (Fig. 3). These upper and lower bounds for diffusion times of 1:1 tau-tubulin complexes were established by measuring the diffusion times of the longest (P1234R′) and shortest (P13) tau constructs used in this study under conditions of excess unlabeled tau (20 μM) and limiting labeled tubulin (20 nM), as described above (Fig. 2). The dashed line and solid line in Fig. 3 are the median diffusion times from the measurements of P13 and P1234R′, respectively. If the truncation constructs form 1:1 tau-tubulin complexes, then their diffusion times are expected to fall within the boundaries set by these lines.

For constructs that include IR$_{2/3}$ or R3, a significant fraction of the diffusion times for the tau-tubulin complexes formed by the truncation constructs are larger than the bounds of these 1:1 tau-tubulin complexes (Fig. 3). Thus, whereas the median diffusion times of the tau-tubulin complexes formed by the truncation constructs are smaller than those of the P1234R′-tubulin complexes, they exceed boundaries set by 1:1 complexes and reflect an average stoichiometry >1:1. In contrast, the diffusion times of P12 are very narrowly distributed around the lower 1:1 tau-tubulin complex boundary (*dashed line*) (Fig. 3; Table 1), suggesting the microtubule binding core of 4R tau binds to tubulin stoichiometrically. The results from these constructs highlight the importance of IR$_{2/3}$–R3 in binding tubulin; when this subdomain is present, some fraction of tau binds multiple tubulin dimers, in good agreement with our previous observations (15).

R2 and R3 contain distinct binding sites for tubulin

A broadly similar trend is observed with P134R′ (Fig. 3), the corresponding three-repeat tau construct of P1234R′. For this construct, stepwise truncation is carried out from R′ to the proposed microtubule binding core, P13 (13). Removal of R′ results in a large drop in both the median diffusion time and peak width to 0.65 and 0.08 ms, respectively, from 0.79 to 0.23 ms. This change reflects both a decrease in the heterogeneity and average size of the diffusing complex. Deletion of R4 does not result in a significant change in either diffusion time or standard deviation (Fig. 3; Table 1). However, the diffusion time of the shortest 3R construct, P13, further decreases to 0.60 ms, comparable to that of the corresponding 4R construct P12, and to the 1:1 P13-tubulin complex formed in the presence of excess tau (Table 1).

FCS measurements of tau constructs with three binding repeats show that those containing both IR$_{1/2}$–R2 and IR$_{2/3}$–R3 (P123 and P132) form complexes with median diffusion times of 0.69 and 0.72 ms, whereas complexes formed by those constructs containing only one of these (P134 contains IR$_{2/3}$–R3, P124 contains IR$_{1/2}$–R2) have median diffusion times of ~0.65 ms (Fig. 4). Interestingly, whether these regions appear in their native order (P123, P134) or scrambled (P132, P124) does not appear to impact multiple tubulin dimer binding. This is reinforced by measurements of native and scrambled four-repeat constructs, all of which contain both IR$_{1/2}$–R2 and IR$_{2/3}$–R3, and where no significant difference between the median diffusion times is observed (Fig. 4; Table 1). Moreover, all of the four-repeat constructs and the three-repeat constructs containing both IR$_{1/2}$–R2 and IR$_{2/3}$–R3 have wider distributions of diffusion times, reflecting greater heterogeneity in these complexes (Fig. 4; Table 1). The fact that the median diffusion times of these complexes exceed the boundaries for 1:1 complex formation reflects that many of the traces result from tau-tubulin complexes with a >1:1 stoichiometry. By contrast, the P134 and
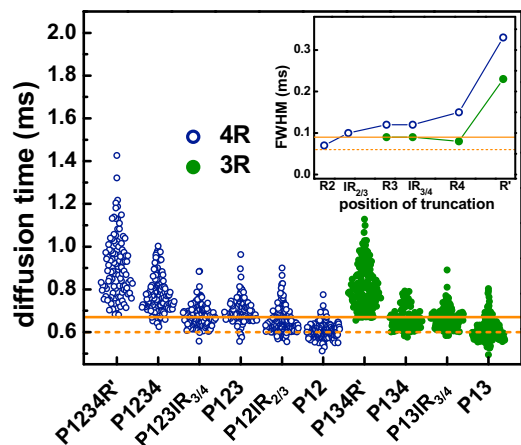

FIGURE 3 Quantification of heterogeneity of tau-tubulin complexes. Diffusion times of tau-tubulin complexes for constructs based on truncation of 4R and 3R tau are plotted. The lines at 0.60 and 0.67 ms denote the upper (*solid*) and lower (*dashed*) boundaries of expected median diffusion times of 1:1 tau-tubulin complexes determined by FCS measurements with excess P1234R′ and P13, respectively, as described in the text. (*Inset*) The widths of Gaussian fits of each distribution of diffusion times are shown. The lines are full width half-maximum from the measurements corresponding to the lines of median diffusion times in the main plot. Details are in the text and Supporting Material. To see this figure in color, go online.
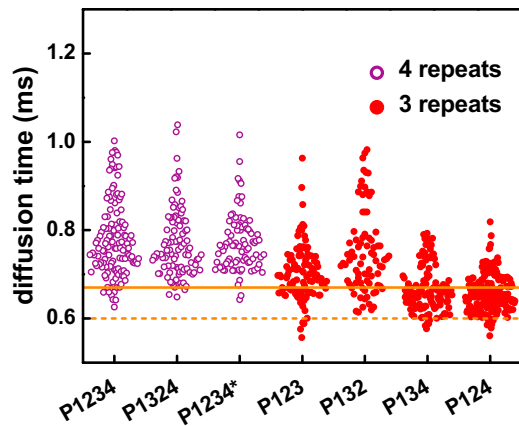
FIGURE 4 Tubulin binding sites in R2 and R3. Diffusion times are plotted of tau-tubulin complexes formed by tau constructs containing either four or three microtubule binding repeats. The solid and dashed lines denote the upper and lower boundaries, respectively, of 1:1 tau-tubulin complexes as described in the text and in Fig. 3. The four-repeat series, in which all constructs contain both $IR_{1/2}$–R2 and $IR_{2/3}$–R3, bind with a >1:1 stoichiometry and significant heterogeneity. In the three-repeat series, only P123 and P132 bind with >1:1 stoichiometry. Constructs lacking either $IR_{1/2}$–R2 (P134) or $IR_{2/3}$–R3 (P124) have smaller median diffusion times, reflecting smaller complexes and lower stoichiometry. To see this figure in color, go online.

FIGURE 5 Correlation between diffusion times and polymerization rates. The inverse of polymerization half-time (k_{obs}) for each construct is plotted against the median diffusion time for each construct. The error bars indicate standard deviations in the rate of polymerization. The solid and dashed lines denote the upper and lower boundaries, respectively, for the median diffusion time of 1:1 tau-tubulin determined using labeled tubulin as described in the text and Supporting Material. To see this figure in color, go online.

P124—each containing only one of these subdomains—form complexes with median diffusion times more consistent with 1:1 stoichiometry. As a whole, the results of these measurements demonstrate that $IR_{1/2}$–R2 and $IR_{2/3}$–R3 are important for binding multiple tubulin dimers and contribute to the heterogeneity of tau-tubulin complexes.

Heterogeneity in tau-tubulin complexes modulates tau function

A subset of the tau constructs to represent the variable types of tubulin complex formation was selected and in vitro tubulin polymerization kinetics were measured by light scattering. The observed rate constant of microtubule polymerization is plotted against the median diffusion time of the tau-tubulin complexes in Fig. 5. The constructs that formed ~1:1 tau-tubulin complexes (bounded by *solid* and *dashed straight lines*, which are the same as in Figs. 3 and 4) polymerize tubulin relatively slowly and invariantly. Once this binding threshold is exceeded, there is a roughly linear relationship between the diffusion time and the observed polymerization kinetics. These results indicate that the ability to bind to multiple tubulin dimers significantly enhances tau's function as a promoter of microtubule polymerization.

Heterogeneity arises from infrequent sampling of cross-linked tau-tubulin complexes

High variability in autocorrelation curves is unexpected in FCS measurements. Within a 10-s measurement of a
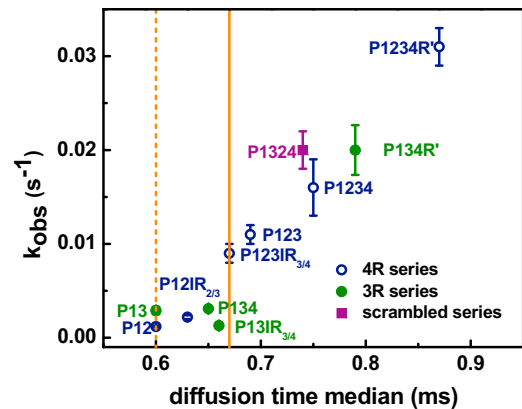
20 nM fluorescent sample, ~200,000 molecules are sampled. Even with a very heterogeneous distribution of tau-tubulin complexes (complexes consisting of tau and a variable number of tubulins), the sampling is sufficient that repeated 10 s autocorrelation curves are expected to be superimposable. To determine the source of the heterogeneous curves, we analyzed time traces of P1234R′ and P13 in the presence of excess tubulin. Only in the case of P1234R′ were bright bursts observed in the traces (Figs. S5 and S6), at a rate of ~0.2–0.6 s⁻¹ (see Supporting Material for details of analysis). Their relative infrequency results in insufficient sampling for population averaging within a 10 s autocorrelation curve. Because tau is the only fluorescent species in these experiments, then the bursts correspond to the diffusion of larger tau-tubulin complexes, cross-linked by tau. The addition of 500 mM KCl to the samples completely eliminates the complexes, with the fluorescent time traces indistinguishable from tau in solution (where no bursts are observed) (Figs. S5 and S6). Our results here, as well as our previous work (15), support multiple binding sites for tubulin within tau. It is not terribly surprising that tau-mediated cross-linking occurs between tau-tubulin complexes. Tau may be associated with single or multiple tubulin dimers, but still have unoccupied binding sites that enable the cross-linking with another tau-tubulin complex. Notably, our observation also requires that tubulin dimers themselves have multiple binding sites for tau. We do not observe tau assemblies in the absence of tubulin (Fig. S1), supporting tau-tubulin-mediated complex formation, as opposed to a tau-tau interaction. Moreover, these dynamic assembles appear to play a role in the initiation of microtubule formation, as they are formed

with greater frequency by tau constructs that polymerize tubulin more rapidly (Fig. 5).

DISCUSSION

Tau's intrinsic disorder poses a challenge to determining the molecular details of its mechanism of function. Moreover, the historic focus on tau's impact on microtubule dynamics and stabilization that does not take into account the role of tau binding to soluble tubulin means that even fundamental aspects of tau function are not well understood. Here we leverage FCS to investigate the heterogeneous complexes tau forms upon binding to soluble tubulin and demonstrate a functional role for these complexes in tubulin polymerization.

Heterogeneity in the stoichiometry of tau-tubulin complexes arises from R′. This is seen both in the large diffusion time—reflecting the presence of complexes with >1:2 tau-tubulin stoichiometry when compared to RB3-tubulin—as well as the significant spread in the diffusion times, reflecting the size heterogeneity in the complexes observed. Moreover, the frequency of cross-linking between tau-tubulin complexes is higher when R′ is present. To a lesser extent, the presence of more repeat regions also contributes to the formation of heterogeneous complexes; in the absence of R′, only constructs that contain all four repeats show large diffusion times and increased heterogeneity. Interestingly, so long as the four repeats are present, their order appears to be unimportant, as scrambled constructs reflect similar degrees of heterogeneity as the native P1234 (Fig. 4).

Distinct tubulin binding sites in $IR_{1/2}$–R2 and $IR_{2/3}$–R3 allow for simultaneous binding of multiple tubulins. For constructs containing only three binding repeats, both of these subdomains must be present for complexes with an average stoichiometry >1:1 to be observed (Fig. 4). The presence of these regions and not their order, appears to be the more important feature, as complexes formed by both P123 and P132 have comparable diffusion times and heterogeneity (Fig. 4). This observation is of particular relevance in that it strongly supports a model where tau binds to tubulin via short sequences within the MTBR, which does not depend upon repeat order (10,25). It is also consistent with our recent study that used single molecule FRET to map topological features of tau in tau-tubulin complexes and found that local conformational changes in the repeats were decoupled from the overall conformational properties of the MTBR, suggesting binding interfaces were localized to discrete regions within the repeats (24).

Many intrinsically disordered proteins retain a significant degree of disorder upon binding to their partners, resulting in polymorphism of the structures of the complexes formed (26,27). This is often the result of multiple individual binding sites consisting of short stretches of amino acids, which may not all interact directly with the binding partner at all times, but nevertheless contribute to the overall binding interaction (28). Such complexes have been labeled "fuzzy", a descriptive term that reflects both their heterogeneity and their dynamic nature (26,29). "Fuzzy" has been used to describe short folded binding sites connected by disordered linkers as seen in binding between Ste5p and Fus3p (30) as well as complexes where disorder persists after binding, such as found in the oligomerization of T-cell receptor ζ-chain (31) or assembly of tropoelastin (32). Perhaps the most similar previously described fuzzy complex compared to what we observe for tau-tubulin is formed by the interaction between the transcriptional activation domain of Ewing's Sarcoma Fusion Protein and its binding target. Ewing's Sarcoma Fusion Protein has multiple, weak binding sites that contain tyrosines that serve as hotspots for recognizing its binding target, whereas the majority of the backbone remains disordered (33,34). Based on the results of this study, tau-tubulin complexes exhibit characteristics consistent with classification as "fuzzy"; tau remains largely disordered upon binding to tubulin (16,24,25,35) and contains multiple binding sites of variable affinities (12,13) that interact with tubulin in a manner that does not appear to be strongly depending upon the order of the sites. Moreover, although we did not directly probe the kinetics of tau-tubulin binding with our measurements, dynamic interchange of tubulin might be expected for fuzzy tau-tubulin complexes and could contribute to the observed heterogeneity.

One of our most intriguing observations is that R′ enhances the fuzziness of tau-tubulin complexes (Fig. 3). Residues 369–386, which span most of R′, are highly evolutionary-conserved, suggesting that R′ has a critical role in tau function (36), distinct from the MTBR. Electrostatic attraction between tau's positively charged MTBR and the negatively charged surface/C-terminal tail of tubulin is thought to be a driving force in their interaction (11,37). The fact that the tau-mediated cross-linking associated with R′ is reversed by the addition of salt, which supports electrostatics-driven assembly. Compared to the repeats, the conserved sequence in R′ has a larger fraction of charged residues and a higher net positive charge per residue (Table S2). More relevant is that the positively charged residues in R′ are generally clustered within a 5–6 residue span forming potential interaction motifs for binding tubulin. These are separated by single negatively charged residues, reflected by a low charge segregation parameter κ (38) (Supporting Material; Table S2 for details). This pattern is well contrasted with R4, where positively charged residues are balanced by negatively charged residues in close proximity, resulting in a neutral net charge, and elimination of potential recognition motifs. The fact that net positive charges in R′ are evenly distributed into separate motifs may allow tubulin to select between adjacent hotspots in R′ stochastically during binding, explaining why the presence of R′ gives rise to significant heterogeneity in tau-tubulin complexes. There are several disease-linked mutations to tau that change the charge distribution within R′, including K369I, E372G, and G389R (39–42), and evidence that these mutants display altered dynamics on the microtubule lattice (36).

The formation of fuzzy complexes appears to be critical to tau function as illustrated by the correlation we observe between increased heterogeneity of tau-tubulin complexes and increased rate of microtubule polymerization (Fig. 5). Constructs that bind to tubulin with an average stoichiometry of ~1:1 are significantly less capable of promoting microtubule assembly. Mechanistically, it may be that constructs that form 1:1 complexes stabilize the weakly attached tubulin dimers in the microtubule lattice in a manner similar to another MAP, XMAP215 (43). Constructs that bind to multiple tubulin dimers, utilizing hot spots both in the MTBR and in R′, significantly enhance the possibility of cross-linking across the microtubule lattice longitudinally or laterally. Moreover, these constructs may also serve as tubulin recruiters, increasing the local concentration of tubulin to facilitate microtubule nucleation and/or polymerization (Fig. 6). It was previously observed that tau fragments comparable to P1234R′ and P134R′ are capable of bundling microtubules (7). Drawing a parallel to the work described here, bundling may also require tau to work as a cross-linker between microtubule assemblies.

CONCLUSIONS

In this work we have characterized the contribution of the inter-repeat/repeat and pseudo-repeat sequences to the formation of tau-tubulin complexes. We demonstrate that tau-tubulin forms heterogeneous, fuzzy complexes mediated primarily by the pseudo-repeat region. Additional, distinct binding sites in R2 and R3 contribute to a lesser extent. We observe a positive correlation between increased binding stoichiometry and the rate of microtubule polymerization, demonstrating functional implications for fuzzy complex formation. A model is proposed that provides mechanistic
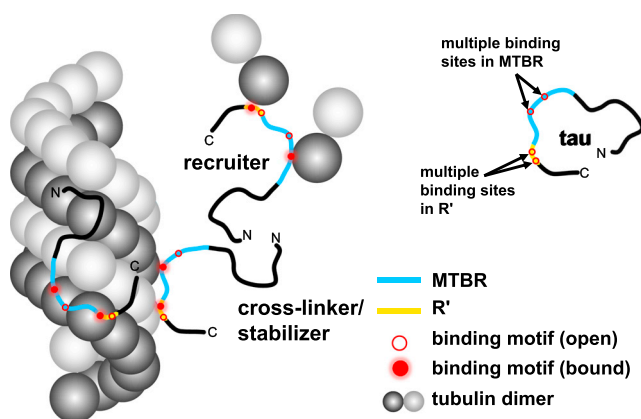
insight into tau function as well into differences between 3R and 4R isoforms of tau. It has long been known that increasing the number of repeats in tau increases its affinity for microtubules (10) and modifies the dynamics of microtubule polymerization (7–9,13). Our results here demonstrate that microtubule dynamics may also be altered by differential stoichiometries of tau-tubulin complexes. Importantly, changes in stoichiometry—and thus changes in function— may arise not only between the naturally occurring 3R and 4R tau isoforms, but perhaps also as a result of mutation or aberrant phosphorylation in disease.

SUPPORTING MATERIAL

AUTHOR CONTRIBUTIONS

X.-H.L. and E.R. designed research. X.-H.L. performed research. X.-H.L. and E.R. analyzed data. X.-H.L. and E.R. wrote the manuscript.

ACKNOWLEDGMENTS

SUPPORTING CITATIONS

References (44–49) appear in Supporting Material.

REFERENCES

1. Ballatore, C., V. M. Y. Lee, and J. Q. Trojanowski. 2007. Tau-mediated neurodegeneration in Alzheimer's disease and related disorders. *Nat. Rev. Neurosci.* 8:663–672.

2. Mazanetz, M. P., and P. M. Fischer. 2007. Untangling tau hyperphosphorylation in drug design for neurodegenerative diseases. *Nat. Rev. Drug Discov.* 6:464–479.

3. Weingarten, M. D., A. H. Lockwood, …, M. W. Kirschner. 1975. A protein factor essential for microtubule assembly. *Proc. Natl. Acad. Sci. USA.* 72:1858–1862.

4. Drubin, D. G., and M. W. Kirschner. 1986. Tau protein function in living cells. *J. Cell Biol.* 103:2739–2746.

5. Trojanowski, J. Q., and V. M. Y. Lee. 2005. Pathological tau: a loss of normal function or a gain in toxicity? *Nat. Neurosci.* 8:1136–1137.

6. Chen, J., Y. Kanai, …, N. Hirokawa. 1992. Projection domains of MAP2 and tau determine spacings between microtubules in dendrites and axons. *Nature.* 360:674–677.

7. Gustke, N., B. Trinczek, …, E. Mandelkow. 1994. Domains of tau protein and interactions with microtubules. *Biochemistry.* 33:9511–9522.

FIGURE 6 Model of tau-tubulin fuzzy complexes. Tau contains multiple tubulin binding motifs (*red circles*) located in the MTBR (*blue*) and R′ (*yellow*). These motifs bind to tubulin or microtubules stochastically and dynamically. This mode of interaction allows tau to perform functional roles as a stabilizer, cross-linker, and recruiter. Variable combinations of binding motifs work cooperatively to stabilize microtubule and promote microtubule assembly.

8. Trinczek, B., J. Biernat, …, E. Mandelkow. 1995. Domains of tau protein, differential phosphorylation, and dynamic instability of microtubules. *Mol. Biol. Cell.* 6:1887–1902.

9. Goode, B. L., P. E. Denis, …, S. C. Feinstein. 1997. Functional interactions between the proline-rich and repeat regions of tau enhance microtubule binding and assembly. *Mol. Biol. Cell.* 8:353–365.

10. Butner, K. A., and M. W. Kirschner. 1991. Tau protein binds to microtubules through a flexible array of distributed weak sites. *J. Cell Biol.* 115:717–730.

11. Mukrasch, M. D., M. von Bergen, …, M. Zweckstetter. 2007. The "jaws" of the tau-microtubule interaction. *J. Biol. Chem.* 282:12230–12239.

12. Goode, B. L., and S. C. Feinstein. 1994. Identification of a novel microtubule binding and assembly domain in the developmentally regulated inter-repeat region of tau. *J. Cell Biol.* 124:769–782.

13. Goode, B. L., M. Chau, …, S. C. Feinstein. 2000. Structural and functional differences between 3-repeat and 4-repeat tau isoforms. Implications for normal tau function and the onset of neurodegenerative disease. *J. Biol. Chem.* 275:38182–38189.

14. Elbaum-Garfinkle, S., G. Cobb, …, E. Rhoades. 2014. Tau mutants bind tubulin heterodimers with enhanced affinity. *Proc. Natl. Acad. Sci. USA.* 111:6311–6316.

15. Li, X.-H., J. A. Culver, and E. Rhoades. 2015. Tau binds to multiple tubulin dimers with helical structure. *J. Am. Chem. Soc.* 137:9218–9221.

16. Kadavath, H., R. V. Hofele, …, M. Zweckstetter. 2015. Tau stabilizes microtubules by binding at the interface between tubulin heterodimers. *Proc. Natl. Acad. Sci. USA.* 112:7501–7506.

17. Gigant, B., I. Landrieu, …, G. Lippens. 2014. Mechanism of Tau-promoted microtubule assembly as probed by NMR spectroscopy. *J. Am. Chem. Soc.* 136:12615–12623.

18. Castoldi, M., and A. V. Popov. 2003. Purification of brain tubulin through two cycles of polymerization-depolymerization in a high-molarity buffer. *Protein Expr. Purif.* 32:83–88.

19. Holehouse, A. S., R. K. Das, …, R. V. Pappu. 2017. CIDER: resources to analyze sequence-ensemble relationships of intrinsically disordered proteins. *Biophys. J.* 112:16–21.

20. Pecqueur, L., C. Duellberg, …, M. Knossow. 2012. A designed ankyrin repeat protein selected to bind to tubulin caps the microtubule plus end. *Proc. Natl. Acad. Sci. USA.* 109:12011–12016.

21. Gigant, B., P. A. Curmi, …, M. Knossow. 2000. The 4 Å x-ray structure of a tubulin:stathmin-like domain complex. *Cell.* 102:809–816.

22. Ravelli, R. B. G., B. Gigant, …, M. Knossow. 2004. Insight into tubulin regulation from a complex with colchicine and a stathmin-like domain. *Nature.* 428:198–202.

23. Barbier, P., A. Dorléans, …, J. M. Andreu. 2010. Stathmin and interfacial microtubule inhibitors recognize a naturally curved conformation of tubulin dimers. *J. Biol. Chem.* 285:31672–31681.

24. Melo, A. M., J. Coraor, …, E. Rhoades. 2016. A functional role for intrinsic disorder in the tau-tubulin complex. *Proc. Natl. Acad. Sci. USA.* 113:14336–14341.

25. Kadavath, H., M. Jaremko, …, M. Zweckstetter. 2015. Folding of the tau protein on microtubules. *Angew. Chem. Int. Ed. Engl.* 54:10347–10351.

26. Tompa, P., and M. Fuxreiter. 2008. Fuzzy complexes: polymorphism and structural disorder in protein-protein interactions. *Trends Biochem. Sci.* 33:2–8.

27. Mukrasch, M. D., S. Bibow, …, M. Zweckstetter. 2009. Structural polymorphism of 441-residue tau at single residue resolution. *PLoS Biol.* 7:e34.

28. Mittag, T., S. Orlicky, …, J. D. Forman-Kay. 2008. Dynamic equilibrium engagement of a polyvalent ligand with a single-site receptor. *Proc. Natl. Acad. Sci. USA.* 105:17772–17777.

29. Fuxreiter, M., and P. Tompa. 2012. Fuzzy complexes: a more stochastic view of protein function. *In* Fuzziness: Structural Disorder in Protein Complexes. Springer, New York, NY, pp. 1–14.

30. Bhattacharyya, R. P., A. Reményi, …, W. A. Lim. 2006. The Ste5 scaffold allosterically modulates signaling output of the yeast mating pathway. *Science.* 311:822–826.

31. Sigalov, A., D. Aivazian, and L. Stern. 2004. Homooligomerization of the cytoplasmic domain of the T cell receptor ζ chain and of other proteins containing the immunoreceptor tyrosine-based activation motif. *Biochemistry.* 43:2049–2061.

32. Pometun, M. S., E. Y. Chekmenev, and R. J. Wittebort. 2004. Quantitative observation of backbone disorder in native elastin. *J. Biol. Chem.* 279:7982–7987.

33. Lee, K. A. W. 2007. Ewings family oncoproteins: drunk, disorderly and in search of partners. *Cell Res.* 17:286–288.

34. Ng, K. P., G. Potikyan, …, K. A. W. Lee. 2007. Multiple aromatic side chains within a disordered structure are critical for transcription and transforming activity of EWS family oncoproteins. *Proc. Natl. Acad. Sci. USA.* 104:479–484.

35. Devred, F., P. Barbier, …, V. Peyrot. 2004. Tau induces ring and microtubule formation from $\alpha\beta$-tubulin dimers under nonassembly conditions. *Biochemistry.* 43:10520–10531.

36. Niewidok, B., M. Igaev, …, R. Brandt. 2016. Presence of a carboxy-terminal pseudorepeat and disease-like pseudohyperphosphorylation critically influence tau's interaction with microtubules in axon-like processes. *Mol. Biol. Cell.* 27:3537–3549.

37. Lefèvre, J., K. G. Chernov, …, P. Savarin. 2011. The C terminus of tubulin, a versatile partner for cationic molecules: binding of Tau, polyamines, and calcium. *J. Biol. Chem.* 286:3065–3078.

38. Das, R. K., and R. V. Pappu. 2013. Conformations of intrinsically disordered proteins are influenced by linear sequence distributions of oppositely charged residues. *Proc. Natl. Acad. Sci. USA.* 110:13392–13397.

39. Neumann, M., W. Schulz-Schaeffer, …, H. A. Kretzschmar. 2001. Pick's disease associated with the novel Tau gene mutation K369I. *Ann. Neurol.* 50:503–513.

40. Tacik, P., M. A. DeTure, …, N. Kouri. 2016. FTDP-17 with pick body-like inclusions associated with a novel tau mutation, p.E372G. *Brain Pathol.* http://dx.doi.org/10.1111/bpa.12428.

41. Murrell, J. R., M. G. Spillantini, …, M. Goedert. 1999. Tau gene mutation G389R causes a tauopathy with abundant pick body-like inclusions and axonal deposits. *J. Neuropathol. Exp. Neurol.* 58:1207–1226.

42. Ghetti, B., J. R. Murrell, …, M. Goedert. 2000. Progress in hereditary tauopathies: a mutation in the tau gene (G389R) causes a Pick disease-like syndrome. *In* Molecular Basis of Dementia. J. H. Growdon, R. J. Wurtman, S. Corkin, and R. M. Nitsch, editors. Wiley, New York, pp. 52–62.

43. Brouhard, G. J., J. H. Stear, …, A. A. Hyman. 2008. XMAP215 is a processive microtubule polymerase. *Cell.* 132:79–88.

44. Hyman, A., D. Drechsel, …, T. Mitchison. 1991. Preparation of modified tubulins. *In* Methods in Enzymology. B. V. Richard, editor. Academic Press, Cambridge, UK, pp. 478–485.

45. Levy, S. F., A. C. Leboeuf, …, S. C. Feinstein. 2005. Three- and four-repeat tau regulate the dynamic instability of two distinct microtubule subpopulations in qualitatively different manners. Implications for neurodegeneration. *J. Biol. Chem.* 280:13520–13528.

46. Hawkins, T. L., M. Mirigian, …, J. L. Ross. 2012. Perturbations in microtubule mechanics from tubulin preparation. *Cell. Mol. Bioeng.* 5:227–238.

47. Huang, N.-P., R. Michel, …, N. D. Spencer. 2001. Poly(l-lysine)-g-poly(ethylene glycol) layers on metal oxide surfaces: surface-analytical characterization and resistance to serum and fibrinogen adsorption. *Langmuir.* 17:489–498.

48. Meseth, U., T. Wohland, …, H. Vogel. 1999. Resolution of fluorescence correlation measurements. *Biophys. J.* 76:1619–1631.

49. Hofmann, H., A. Soranno, …, B. Schuler. 2012. Polymer scaling laws of unfolded and intrinsically disordered proteins quantified with single-molecule spectroscopy. *Proc. Natl. Acad. Sci. USA.* 109:16155–16160.